J. Biophotonics **7**, No. 7, 534–541 (2014) / **DOI** 10.1002/jbio.201300016

Journal of
BIOPHOTONICS

FULL ARTICLE

Imaging directed photothermolysis through two-photon absorption demonstrated on mouse skin – a potential novel tool for highly targeted skin treatment

Hequn Wang[**,1], *Soodabeh Zandi*[**,2], *Anthony M.D. Lee*[1], *Jianhua Zhao*[1,2], *Harvey Lui*[2], *David I. McLean*[2], *and Haishan Zeng*[*,1,2]

[1] Imaging Unit – Integrative Oncology Department, British Columbia Cancer Agency Research Centre, Vancouver, BC, Canada
[2] Photomedicine Institute – Department of Dermatology and Skin Science, University of British Columbia & Vancouver Coastal Health Research Institute, Vancouver, BC, Canada

Received 25 January 2013, revised 20 February 2013, accepted 21 February 2013
Published online 19 March 2013

Key words: two-photon absorption photothermolysis, precise laser-induced tissue alteration, skin, two-photon fluorescence, second-harmonic-generation, multiphoton microscopy, confocal microscopy

One-photon absorption based traditional laser treatment may not necessarily be selective at the microscopic level, thus could result in un-intended tissue damage. Our objective is to test whether two-photon absorption (TPA) could provide highly targeted tissue alteration of specific region of interest without damaging surrounding tissues. TPA based laser treatments (785 nm, 140 fs pulse width, 90 MHz) were performed on *ex vivo* mouse skin using different average power levels and irradiation times. Reflectance confocal microscopy (RCM) and combined second-harmonic-generation (SHG) and two-photon fluorescence (TPF) imaging channels were used to image before, during, and after each laser treatment. The skin was fixed, sectioned and H & E stained after each experiment for histological assessment of tissue alterations and for comparison with the non-invasive imaging assessments. Localized destruction of dermal fibers was observed without discernible epidermal damage on both RCM and SHG + TPF images for all the experiments. RCM and SHG + TPF images correlated well with conventional histological examination. This work demonstrated that TPA-based light treatment provides highly localized intradermal tissue alteration. With further studies on optimizing laser treatment parameters, this two-photon absorption photothermolysis method could potentially be applied in clinical dermatology.

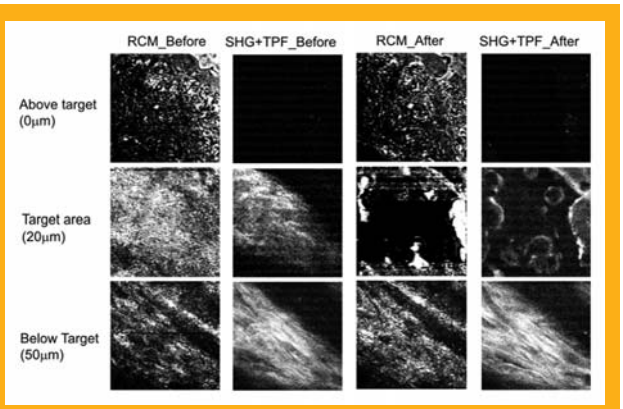

RCM and SHG + TPF images comparing before and after high power fs laser irradiation, demonstrated highly localized tissue alternation.

* Corresponding author: e-mail: hzeng@bccrc.ca, Phone: +1 604067508083, Fax: +1 604 675 8099
** These authors have made equal contributions to this paper.

1. Introduction

Lasers can be used to target skin chromophores such as water, hemoglobin, and melanin to perform fast and precise treatment on a variety of skin lesions [1–2]. Laser therapy generates little discomfort during and after the treatment, and also has lower risk of scarring. Common skin conditions that can be treated using laser therapy include: vascular lesions (port-wine stains, haemangiomas), pigmented lesions (freckles, birthmarks, nevi), tattoos, unwanted facial or body hair, facial wrinkles, sun-damaged skin, keloids, hypertrophic scars, and skin cancers [3–5].

Traditional laser treatment, which is essentially an one-photon absorption process, has chances of causing unintended tissue damage at microscopic level. For example, if the targeted chromophore is the melanin inside dermis, by focusing the laser beam onto the targeted melanin, the untargeted melanin inside epidermis will highly likely to be damaged as well due to the absorption to the laser light. This scenario is relevant for laser treatment of dermal tumors, hirsutism, hyperhidrosis, etc. Two-photon absorption (TPA) is a process where two longer wavelength (near-infrared) photons get absorbed simultaneously by a molecule, and it only occurs at the focal point. This provides the possibility of highly targeted tissue alteration of specific dermal structures without damaging structures in the epidermis, and may potentially solve the problem in the one-photon laser treatment. Interestingly, during the TPA process, there are natural fluorophores inside the skin, such as keratin, NADH, melanin, and elastin, which can emit two-photon excitation fluorescence (TPF), while non-centrosymmetric structures such as collagen, can produce second-harmonic-generation (SHG) signals [6]. This leads to high biochemical specificity detection. Therefore, TPF and SHG signals can be used to image before and after the two-photon laser-induced tissue alteration, and also for monitoring tissue alteration during the high power irradiation. More advantages of two-photon excitation include its inherent optical sectioning capability, deeper penetration depth, less photo-damage and photo-bleaching of the non-focused areas on the beam path. We hypothesize that TPA from the skin will provide precise damage to targeted skin structures by inducing two-photon absorption photothermolysis.

The exploration of two-photon absorption based laser therapies has been growing recently. Two-photon photodynamic therapy has been demonstrated using NIR femtosecond (fs) pulses [7]. It is a photo-chemical process which involves using two-photon absorbing dye as a photosensitizer, and is mainly used in cancer treatment. To evaluate two-photon based photo-thermal effects, an YB: KYW femtosecond (fs) laser has been used to ablate porcine corneal samples. Ablation thresholds were also determined using three diode pumped solid-state ultrafast lasers. It was found that corneal ablation threshold remained almost constant within the first 200 μm of stroma and was proportional to the square root of the laser pulse width [8]. The relationships between the fs laser pulse length, power density, pulse number, and the cornea excision quality as well as the resulting tissue morphologies have also been studied using visible laser wavelengths [9]. However, to our knowledge, there has been no published study on TPA based laser treatment on skin.

Therefore, the objective of this study is to explore the feasibility of two-photon laser absorption for targeted skin modification. We believe that two-photon laser absorption for targeted skin alteration may potentially be used to precisely treat dermal tumors, hirsutism, hyperhidrosis, and birthmarks without damaging the surrounding normal skin or causing scars. Here, we present a preliminary study on TPA based tissue alteration on mouse skin, and we hope this idea can one day be used as a skin treatment tool and be adapted into clinic.

2. Experimental

2.1 Animal preparation

Skin excised from the shaved backs of euthanized female C3H/HeN mice ($N = 10$) was used in this study. The skin was oriented on a glass slide with the epidermal side up and then covered with a glass coverslip. Distilled water was added in between the coverslip and the microscope objective for refractive index matching. All animal experiments were performed according to a protocol approved by the University of British Columbia Committee on Animal Care (certificate #: A10–0338).

2.2 Integrated reflectance confocal microscopy and two-photon imaging system

Our home-made integrated reflectance confocal (RCM) and multiphoton microscopy (MPM) system was used for the laser treatment experiment and for imaging guidance and monitoring. Details of the system can be found elsewhere [10]. Briefly a tunable, fs Ti: Sapphire laser (720–950 nm, 140 fs pulsewidth, 90 MHz, Chameleon, Coherent Inc., Santa Clara, California) was used as the excitation source for both the tissue alteration and the imaging monitoring. To improve both the illumination and detection efficiency, the 50/50 beamsplitter used in the previous

system was replaced with a polarization beamsplitter (PBS) along with a quarter waveplate to effectively direct both the illumination laser beam to the sample and the de-scanned reflectance confocal signals to the RCM detector. The illumination laser beam was circular-polarized, directed into a 60X (NA = 1.0) water-immersion microscope objective, and focused onto the skin. The laser spot at the skin was scanned using two scanners to generate the RCM and SHG + TPF images with a speed of 0.067 second per frame (15 frames/s). Both TPF and SHG signals were collected onto a single photon detector hereinafter referred to as the SHG + TPF imaging channel. The RCM and SHG + TPF images were recorded by a frame grabber as synchronized independent video streams. As both the RCM and SHG + TPF imaging channels share the same laser, scanners, and microscope objective, the RCM and SHG + TPF images are perfectly registered [9]. A polarizer-$\lambda/2$ waveplate combination at the laser exit was used to adjust the incident laser power at the sample to be 30 mW for imaging, and 75 mW or 200 mW for tissue alteration/treatment. The wavelength used for both imaging and tissue alteration was 785 nm. This wavelength was selected because: (1) it falls within the tissue optical "window", where the one-photon absorption of light by tissue is minimized and tissue penetration depth is maximized; (2) it matches the wavelength of our existing CW laser that will be used in the CW and fs laser comparison experiment. TPA at 785 nm corresponds to the one-photon absorption in the UV wavelength range, which has been employed in conventional one-photon phototherapy due to strong tissue absorption.

In order to target at different depths, the microscope objective was mounted on a piezoelectric scanner (MIPOS 500 SG, Piezosystem Jena, Jena, Germany) that allows up to 400 μm of closed-loop travel. Coarse adjustment of the scanning area was achieved using a manually actuated 3-axis translational stage.

Both RCM and SHG + TPF images were acquired before and after the tissue alteration at the targeted skin layers as well as at vertical levels of 0 μm and 60 μm depth within the skin. For all the tissue alteration processes, 0 μm depth was defined as the layer where the uppermost stratum corneum just can be found in the RCM imaging channel. During the high power treatment irradiation, RCM and SHG + TPF were also used to monitor the damaging process. In total, 20 pieces of mouse skin were imaged and treated. Three different target depths beneath the skin surface (20, 30, and 40 μm) and three different exposure times (from 0.5 to 3 min) were tested to study the effects of target depth and irradiation period on tissue alteration efficacy (Table 1).

Figure 1 illustrates the horizontal views of the skin sample (X–Y plane is parallel to the skin surface, Z represents the depth into the skin). The skin sample blocks are 5 mm × 10 mm size. In order to orient and localize the target damaged sites for subsequent histologic analysis we initiated the irradiation processes over areas of 150 μm × 150 μm at 1 mm away from one of the long edges of each sample (Figure 1b). Then, following the irradiation parameters for each specimen group, we moved 150 μm along the Y-axis to treat the adjacent area

Table 1 Combinations of target depth and laser exposure duration.

Skin sample #	1–3	4–5	6–7	8–9	10	11–13	14–16	17–18	19–20
Target depth (μm)	20	30	30	30	30	40	40	40	40
Irradiation period (min)	0.5	0.5	1	2	3	0.5	1	2	3

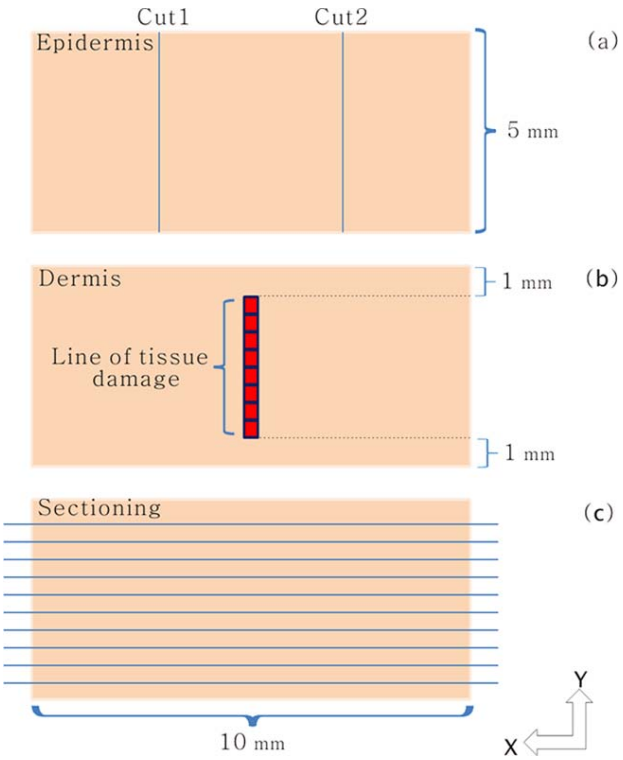

Figure 1 Diagram demonstrating the horizontal view (X–Y plane) of the epidermal cuts, the line of tissue damages at dermis layer, and the histological sectioning. The three skin-colored rectangular blocks represent the horizontal view of the skin samples, which were 5 mmm × 10 mm size. (**a**) Horizontal view of epidermal layer of the skin with two cuts; (**b**) Horizontal view of dermal layer with the line of tissue damage, which consists of several exposure areas shown as red squared blocks; (**c**) Horizontal view of sectioning direction on the X–Y plane. Multiple sections were performed in order to cover the whole line of damage.

(150 μm × 150 μm) at the same depth *Z*. By iterating this process, we were able to create a line of damage along the Y-direction within an X–Y plane at certain depth in the dermis that was 1 mm away from both edges. After each irradiation process, the epidermis was marked twice in parallel to each side of the laser-induced damaging line using a scalpel (Figure 1a). The skin samples were then processed, sectioned, and stained with hematoxylin and eosin (H & E) for histologic examination (Figure 1c). The damage line induced by the high power laser irradiation, the cutting mark lines, and the histological sectioning are schematically illustrated in Figure 1. Figure 1a demonstrates the two epidermal cuts, and Figure 1b shows the line of damage in the dermis with each exposure unit area of 150 μm × 150 μm. The skin samples were sectioned perpendicularly to the epidermal cuts and line of tissue damage. This allowed us to locate the damaged area in the dermis with two epidermal cuts as reference in the histological slides.

In order to test whether the tissue damages generated by the ultrafast fs laser are mainly due to two-photon absorption versus single photon near infrared absorption, a control study using a continuous wave (CW) laser was performed. The CW laser (I0785SA0100B-TK, Innovative Photonics Solutions, Monmouth Junction, New Jersey), which has a central wavelength of 785 nm, was coupled into the combined reflectance confocal microscopy and two-photon imaging system using a flip mirror. This setup allows us to switch between the CW laser source from the fs laser source. The CW laser beam path was optimized to follow the same fs laser beam path, allowing the two laser beams to focus at the same depth within the skin. In this way the reflectance confocal imaging derived from the CW laser was used to monitor the CW laser-induced tissue alteration itself, and SHG + TPF imaging from the fs laser was used before and after the CW irradiation to better evaluate the tissue damages. For the CW laser, the maximum power that can be coupled into the microscope objective was 60 mW. Therefore, in the control experiments, for both the CW and fs laser-induced tissue alterations, the following parameters were the same: 60 mW power, 785 nm wavelength, 30 μm tissue alteration depth, and 70 μm × 70 μm exposure area. For the fs laser-induced tissue alteration experiment, confocal and SHG + TPF images of the skin were acquired before, during and after each high-power irradiation, whereas for the CW laser-induced tissue alteration experiment only CW confocal images were acquired during the tissue treatment process, since there is no SHG + TPF signals generated in the CW mode. Nevertheless paired SHG + TPF images generated from the fs laser and CW confocal images were acquired before and after each high-power irradiation process. We performed this comparison experiment at multiple sites on 3 skin samples.

3. Results and discussion

In order to directly monitor the tissue effects, both RCM and SHG + TPF images were acquired during the high power laser irradiation treatment. In the dermis, the main fluorophore that generates TPF is elastin, and collagen fiber is the structure that generates strong SHG signals. Figure 2a shows a sequence of extracted RCM and SHG + TPF video images at 4 different time points during treatment where the targeted depth was 20 μm. The dermis was intact in both RCM and SHG + TPF imaging channels at 0 s baseline. With 75 mW of power irradiation, dermal fiber alteration first became apparent at 3 s. By 9 s obvious changes were seen in both the RCM and SHG + TPF imaging channels. We believe that during the laser treatment, both elastic and collagen fibers were denatured due to the increased temperature, which accounted for the loss of TPF + SHG signals [11–12]. Figure 2b shows representative RCM and SHG + TPF images comparing before and after targeted treatment as monitored at different tissue depths. Above the targeted layer, the stratum corneum remains qualitatively the same in the RCM imaging channel at the completion of the laser exposure. Below the 20 μm target layer (i.e. at ~50 μm beneath the 0 μm surface reference layer), both RCM and SHG + TPF imaging channels showed strong signals from dermal fibers that were morphologically very similar before and after treatment. At the targeted layer (~20 μm beneath the 0 μm refer-

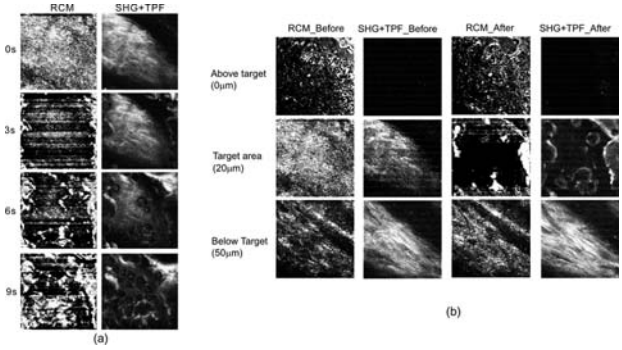

Figure 2 RCM and SHG + TPF images comparing before, during and after high power fs laser irradiation. Laser wavelength: 785 nm, imaging power: 20 mw, irradiation power for tissue alteration: 75 mw, target depth: 20 μm, irradiation period: 0.5 min, both the treatment area and image field-of-view (FOV) are 70 μm × 70 μm. (**a**) RCM and SHG + TPF image frames at 0, 3, 6, and 9 s during the laser irradiation; (**b**) RCM and SHG + TPF images before and after high power irradiation at 0, 20, and 50 μm depths.

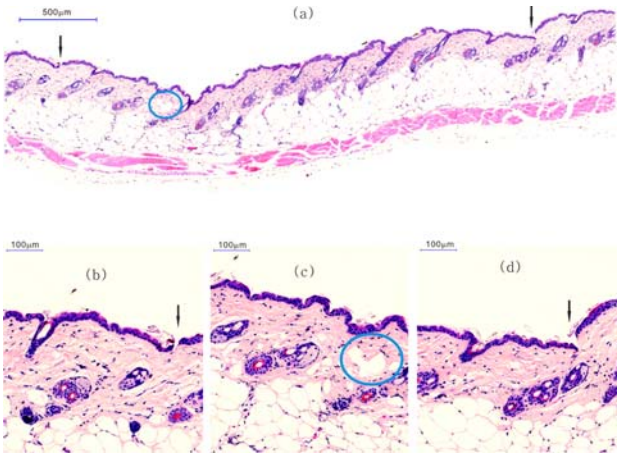

Figure 3 H & E histological photomicrographs demonstrating selective alteration in laser-exposed mouse skin: (**a**) Histology view of the damaged area (indicated by the blue circle) and the two epidermal cuts (indicated by the black arrows). Zoomed-in views of (**b**) left cut (indicated by the black arrow), (**c**) targeted damaged area (indicated by the blue circle), and (**d**) right cut (indicated by the black arrow).

ence layer), fibrous structures were found in both RCM and SHG + TPF images before treatment. During the laser treatment, we found that in contrast to the SHG + TPF imaging channel which shows dark holes within the target layer, the RCM signals were increased in the form of bright structures and focal signal saturations. RCM and SHG + TPF at the level of the targeted skin layer appear different as monitored throughout the laser exposure.

The marked epidermal landmarks (two cuts indicated by black arrows) were found on the hematoxylin and eosin (H & E) stained section shown in Figure 3a. An empty space devoid of dermal fibers measuring approximately 100 μm × 50 μm (inside the blue circle) can be visualized between the two epidermal landmarks and represents the laser target site within the skin. Zoomed-in views of the two landmarks as well as the targeted area are shown in Figure 3b, c, and d, respectively. Around the vicinity where the laser created an empty space, the adjacent epidermis, deeper dermis and subcutaneous fat layers remained intact.

Figure 4 shows SHG + TPF images at different depths comparing before and after the high power (200 mW) laser irradiation with a target depth of 40 μm and a tissue alteration time period of 2 min. No significant structural changes were found at 10, 20, and 30 μm depths. At 40, 50, and 60 μm depths, an empty hole in between the fiber structure was seen.

To explore the correlation between the irradiation period and tissue alteration efficacy, SHG + TPF images at different depths comparing before and

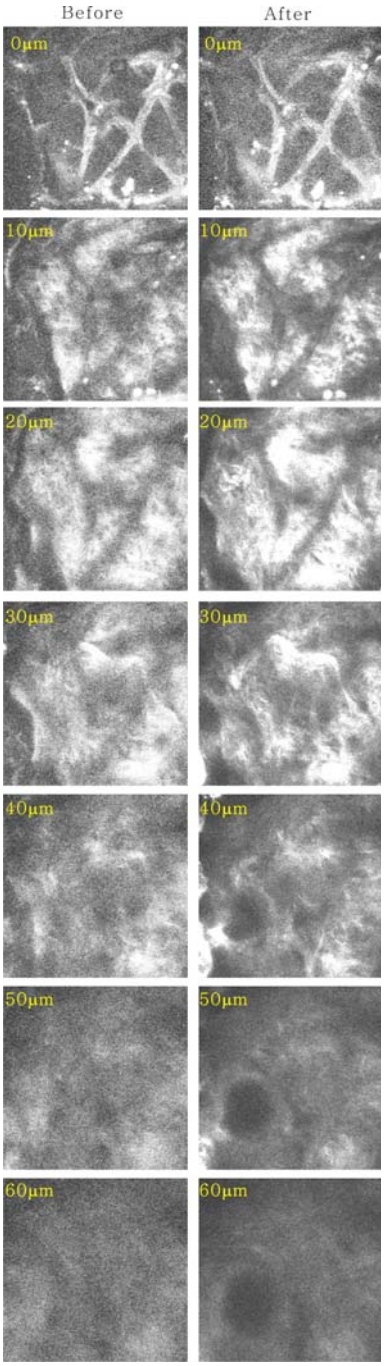

Figure 4 SHG + TPF images of different depths comparing before and after high power (200 mW) laser irradiation with a target treatment depth of 40 μm and a irradiation period of 2 min. The exposure area and the image FOV: 150 μm × 150 μm.

after the procedure with a target depth of 40 μm and irradiation periods of 1 min and 3 min were also acquired (data not shown). For 1 min irradiation period at 40 μm target depth, only very subtle changes were found in the images. However, for 3 min irra-

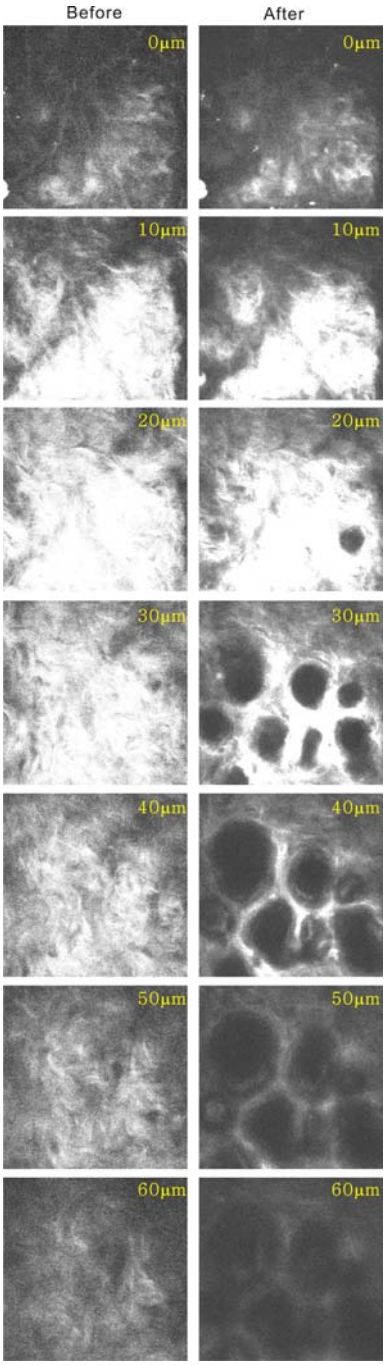

Figure 5 SHG + TPF images of different depths comparing before and after high power (200 mW) irradiation with a target depth of 30 μm and an irradiation period of 2 min. Exposure area and the image FOV: 150 μm × 150 μm.

diation period at 40 μm target depth, much bigger holes in between the dermal fibers were observed at 40, 50, and 60 μm depths with no visible changes at the upper layers.

To determine whether targeting at different depth will have different effects at other depths, high power irradiation targeting at 30 μm beneath the skin surface was also performed. Figure 5 shows SHG + TPF images of different depths comparing before and after the high power (200 mW) laser irradiation with a target of 30 μm and with an irradiation period of 2 min. Significant structural dermal changes were found starting from 20 μm. Multiple holes in between the dermal fibers were observed at depth of 30, 40, 50, and 60 μm. Layers above 20 μm depth were left intact. SHG + TPF images of different depths comparing before and after the procedure targeting 30 μm beneath the surface with an irradiation period of 0.5 min were also acquired (data not shown). Similar effects were observed compared to the results achieved with an irradiation period of 2 min. Dermal changes were found from 20 μm down to 60 μm. Epidermal changes were not observed.

In order to confirm that the tissue alterations generated by fs laser pulses are dominated by two-photon absorption rather than one-photon absorption, a control study using a CW laser was performed. The CW laser irradiation will induce one-photon absorption only. The target depth was selected as 30 μm. Before the high power irradiation, a CW confocal image was taken which is shown in Figure 6 (a-1). Since MPM images are better for demonstrating tissue damage, a SHG + TPF image was also taken before the procedure, which is shown in Figure 6 (a-3). The high power irradiation was performed using the CW laser at 60 mW for an exposure period of 1.5 min, FOV (70 μm × 70 μm). No change in the CW confocal images was found during the irradiation process. As shown in Figure 6 (a-2) and (a-4), intact fiber structures can be seen in both the CW confocal and SHG + TPF images after the procedure. However, with the same target depth (30 μm), wavelength (785 nm), power level (60 mW), FOV (70 μm × 70 μm), and irradiation period (1.5 min), significant dermal fiber damages were found after the fs irradiation. SHG + TPF images at different depths before the irradiation can be found in Figure 6b column (b-1), and the SHG + TPF images after the irradiation are shown in Figure 6b column (b-2). At the target depth of 30 μm, damaged fibers can be seen clearly in the SHG + TPF images. No damage was found at the epidermis (0 μm) and depth of 60 μm. The fs confocal images before and after high power irradiation are shown in Figure 6b column (b-3) and (b-4). Changes at depth of 20 μm, 30 μm, and 40 μm can be found in the confocal images, but with intact epidermis (0 μm) and intact dermal structures at depth of 60 μm. This experiment comparing the fs laser treatment effect with that of the CW laser treatment demonstrated that at 785 nm, the one-photon absorption is weak and has minimum effect on tissue, while the fs laser treatment effect on tissue is indeed caused by strong two-photon absorption.

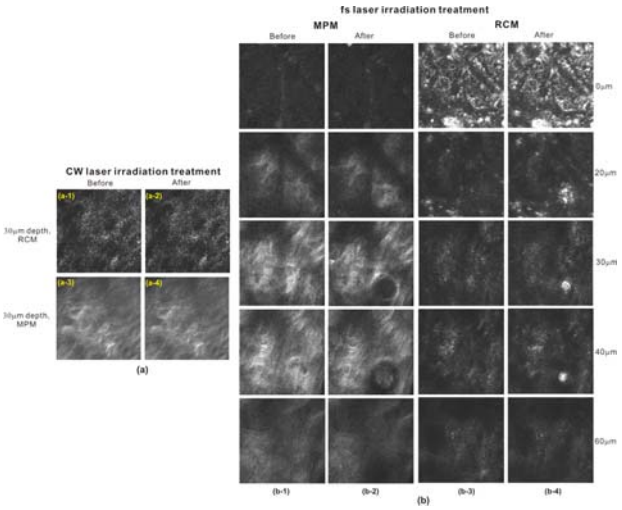

Figure 6 Comparison of CW laser-induced tissue alteration (**a**) and fs laser-induced tissue alteration (**b**). CW confocal images of mouse skin at the target depth of 30 μm showing before high power (60 mW) irradiation (a-1) and after (a-2); SHG + TPF images generated from fs laser at the target depth of 30 μm showing before high power irradiation (a-3) and after (a-4); SHG + TPF images of mouse skin at different depths showing before high power (60 mW) irradiation in column (b-1) and after in column (b-2); fs confocal images of mouse skin at different depths showing before high power irradiation in column (b-3) and after in column (b-4). Exposure area and image FOV: 70 μm × 70 μm.

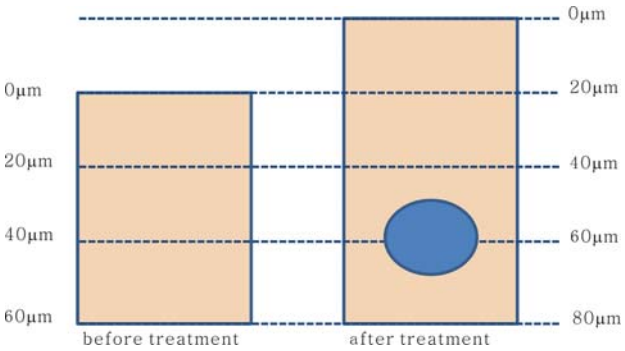

Figure 7 Proposed explanation for tissue elevation during tissue alteration.

Our experiment has clearly demonstrated the advantages of using two-photon absorption based photothermolysis on mouse skin treatment, including highly-targeted tissue alteration and the capability of real-time monitoring through RCM and SHG + TPF. For example, our results have shown that we can target on damaging mouse dermal fibers without affecting epidermal structures. RCM and SHG + TPF imaging channels can provide both morphological and biochemical information of the tissue structure under irradiation, which allow us to monitor the tissue alteration in real time. This feature can also be used to explore optimal tissue alteration efficacy. Moreover, from a clinical treatment point of view, timely stop of the irradiation procedure could be applied with these real-time imaging monitoring. This may potentially prevent incorrect treatment or overtreatment to the skin, therefore making the treatment process more controlled and flexible. Therefore, further improvement on the system performance such as improving the signal-to-noise ratio should be considered. We have noticed that some mouse skin samples, such as the one shown in Figure 2, have very weak signals in the SHG + TPF imaging channel, probably due to the thin stratum corneum and epidermis. Only one layer of cells was found in the histology images, and this could be the reason that we were lack of signals in our SHG + TPF imaging channel in Figure 2.

Interestingly, in Figure 4, we noticed that the biggest diameter of the damaged area was shown at the depth of 60 μm, rather than the target depth at 40 μm. We propose a possible explanation as shown in Figure 7. Compared with before high power laser treatment, the skin could elevate due to the space generated during the procedure. In this case, if 0 μm is still defined as the layer of stratum corneum, the largest diameter of the hole would be at a depth lower than 40 μm. From our experiment, it seems that for the target depth of 40 μm, the tissue elevation was around 20 μm, therefore, the largest diameter of the hole was at 60 μm beneath the surface. For the target depth of 30 μm, the tissue elevation was around 10 μm, and the largest diameter of the hole was located at around the depth of 40 μm, which can be found in Figure 5.

When comparing the tissue alteration results for different target depths, we noticed that the damage threshold for 40 μm was much higher than 20 μm or 30 μm. To be more specific, for target depth at 40 μm, dermal damages were observed starting from 20 s. However, for target depth at 30 μm, dermal damages were found within 10 s of laser irradiation. For target depth at 20 μm, dermal damages were initialized within 3 s of laser irradiation. In addition, for target depth at 30 μm, it seems that the damaging is more likely to affect the skin layer at 10 μm above the targeted layer. No discernable change was found at 10 μm above the targeted layer when the target depth was set to be 40 μm. This may indicate that photothermal effect at deeper depths is more restricted to local area compared with more superficial skin layers due to the structural differences at different depths. Therefore, this two-photon absorption based photothermolysis may be applied better to treat skin lesions at deeper locations.

If the tissue alteration induced by fs laser was predominantly due to NIR one-photon absorption, we should observe similar tissue alteration effects with a

CW laser. Therefore, targeted at the same target depth (30 μm) and with the same wavelength (785 nm), power level (60 mw), FOV (70 μm × 70 μm), and irradiation period (1.5 min), CW laser-induced tissue alteration which represents one-photon absorption situation, and fs laser-induced tissue alteration which represents two-photon absorption situation, were compared. Our results showed that the CW laser failed to generate damaging effects, while significant dermal fiber damages were found during the fs laser irradiation under the same condition. This confirmed that the fs laser-induced highly-targeted tissue alteration that we observed are not due to near IR one-photon absorption, but due to two-photon absorption as we expected. And the two-photon absorption cross-section must be much higher than the one-photon absorption cross-section. This makes sense because the two-photon absorption under 785 nm fs laser excitation corresponds to one-photon absorption at 392.5 nm in the UV range, while the one-photon absorption of 785 nm is at near IR range. It is known that tissue absorption at UV range is much higher than at near IR range. Specifically previous studies have shown that the absorption coefficient of dermis at 400 nm is around ~10 times higher than the absorption coefficient of dermis at 785 nm [13]. This explains why there was no tissue damage found for 785 nm CW laser irradiation. Besides, thermal diffusion was observed during our experiment, which indicates that the tissue ablation is primarily from photothermal effect.

In addition, the absorption coefficient of dermis is very close to the absorption coefficient of epidermis at 400 nm [13]. Being able to damage the dermis without altering the epidermis shown in this study proved that even with similar absorption coefficient, the fs laser induced two-photon absorption based tissue alteration can be very specific. These findings indicate that the two-photon absorption based photothermolysis has great potential to be used as a novel clinical treatment tool.

4. Conclusion

In conclusion, localized destruction of dermal fibers by two-photon absorption photothermolysis was demonstrated in *ex vivo* mouse skin while concurrently not damaging the overlying epidermal tissue nor the tissue below the irradiation layer. RCM and SHG + TPF images correlated well with conventional histologic examination on assessing the tissue alterations. Target depths and irradiation period are important parameters that determine the amount of resulting damage. Micro-structures such as cells, hair follicles, sweat glands and sebaceous gland are very likely to have different changes when performing two-photon based photothermolysis. Therefore, future studies on optimizing laser wavelength, laser power, laser pulse width, target depth and irradiation period for different skin structures of *in vivo* skin should be performed. We believe that two-photon-based light absorption could provide highly localized intradermal tissue alteration and could potentially be used for therapeutic applications in dermatology.

Acknowledgements This work was supported by the Canadian Dermatology Foundation, the VGH & UBC Hospital Foundation, the BC Hydro Employees Community Services Fund, and the BC Cancer Agency. AMDL acknowledges MSFHR and CIHR-SRTC for postdoctoral funding. HW acknowledges CIHR-SRTC for doctoral funding.

Conflict of interest The authors' institution British Columbia Cancer Agency has filed a patent application related to the subject of the manuscript.

Author biographies Please see Supporting Information online.

References

[1] R. R. Anderson and J. A. Parrish, Science **220**, 524–527 (1983).
[2] L. Carroll and T. R. Humphreys, Clin Dermatol **24**, 2–7 (2006).
[3] E. L. Tanzi, J. R. Lupton, and T. S. Alster, J Am Acad Dermatol **49**, 1–31 (2003).
[4] K. A. Jang, E. C. Chung, J. H. Choi, Sung K. J., K. C. Moon, and J. K. Koh, Dermatol Surg **26**, 231–234 (2000).
[5] B. D. Zelickson, S. L. Kilmer, V. A. Chotzen, J. Dock, D. Mehregan, and C. Coles, Lasers Surg Med **25**, 229–236 (1999).
[6] A. M. D. Lee, H. Wang, Y. Yu, S. Tang, J. Zhao, H. Lui, D. I. McLean, and H. Zeng, Opt Lett **36**, 2865–2867 (2011).
[7] J. D. Bhawalkar, N. D. Kumar, C. F. Zhao, and P. N. Prasad, J Clin Laser Med Sur **15**, 201–204 (1997).
[8] H. Sun, M. Han, M. H. Niemz, and J. F. Bille, Lasers Surg Med **39**, 654–658 (2007).
[9] W. Kautek, S. Mitterer, J. Kruger, W. Husinsky, and G. Grabner, Appl Phys A-Mater **58**, 513–518 (1994).
[10] H. Wang, A. M. D. Lee, Z. Frehlick, H. Lui, D. I. McLean, S. Tang, and H. Zeng, J Biophotonics, DOI 10.1002/jbio.201200067 (2012).
[11] T. A. Theodossiou, C. Thrasivoulou, C. Ekwobi, and D. Becker. Biophys J **91**, 4665–4677 (2006).
[12] A. J. Walsh, D. B. Masters, E. D. Jansen, A. J. Welch, and A. Mahadevan-Jansen, Lasers Surg Med **44**, 712–718 (2012).
[13] E. Salomatina, B. Jiang, H. Novak, and A. N. Yaroslavsky, J Biomedical Opt **11**, 0640261–0640269 (2006).